Topological Analysis on the Modulus and Network Structure of Miscible Polymer Blends

Jung Mo Son and Hyungsuk Pak

Department of Chemistry, Seoul National University, Seoul 151-742, Korea
Received October 29, 1994

A topological theory is introduced to extend Tsenoglou's theory to polymer blends having temporary and permanent networks composed of multicomponent polymers which have miscible and flexible chains. The topological theory may estimate the values of free elastic energy, the molecular weight between entanglements, and the equilibrium shear moduli, and it may establish more correctly the topological relations among these physical quantities. Through such introduction of the topological theory, there can be topologically analyzed the mixing law for the rubbery plateau modulus of a fluid polymer blend, and there can be considered the topological relationship to the equilibrium modulus of an interpenetrating polymer network containing trapped entanglements and dangling segments. The theoretically predictive values are compared and show good agreement with the experimental data for several miscible polymer blends.

Introduction

Recently, topological theories have played a great role in studing the elasticity of polymers. The theories which have systematically dealt with rubber elasticity so far are the phantum network theories[1~6] headed by Flory and others and the topological network theories[7~12] headed by Iwata and others. Phantom network theories have retrograded in recent years because of the fact that they have dealt with the energies of rubber elasticity as only functions of the end-to-end distance between chains, and so they have not considered the effect of interaction between chains by entanglement. On the other hand, recently developed topological network theories can explain very well the effect of interaction between chains by entanglement. Iwata has theoretically explained the various phenomena of rubber elasticity by applying topological theories to a polymer system which consists of only a single kind of polymers.[10~12] The models which he has offered are mainly confined to the SCL (simple cubic lattice) models,[11~12] and he did not obtain nor offer detailed transformation matrices and related topological distribution functions about the THL (tetrahedral lattice) model. We offer detailed transformation matrices about the THL model and related topological distribution functions by extending topological theories of Iwata of the THL model (called the BCL model earlier by the previous work[13]), and we analyze the Tsenoglou's theory[14] of polymer blends in view of topological approach. And the question of how free energy of polymer blends, plateau moduli, and molecular weight are bound up with interaction between chains of polymer systems has been systematically examined in detail. Here, a topological theory for polymer blends has been evolved based upon the Tsenoglou's theory under the assumption that all the junction points of polymer blends forms the THL model for some average time interval.

In the present work, the survey of the THL model is concisely described, and the corresponding equations which are related to the THL model are topologically evolved. Then, through the comparison of these topological results with those of the Tsenoglou's,[14] the corresponding physical quantities of the Tsenoglou's theory are analyzed in view of the topological theory by consideration of excluded-volume effects in the given polymer systems. Finally, the theoretically predictive values are compared with the experimental data.

THL Model

This tetrahedral lattice (THL) model has been known as the body-centered cubic lattice (BCL) model.[13] The new name emphasizes the actual structure of the model.

The distribution functions and transformation matrices about the THL model had already been offered originally in the previous work.[13] In the present work, topological theories of polymer blends are evolved by introducing a part of the previous work. The results carried out in this work are such things as the work which applies the distribution functions obtained from the THL model to the Tsenoglou's statistical theory and as the work which explains the previous experimental results reasonably by obtaining the values of free energy, distribution functions, molecular weight, and plateau moduli. From now on, the structure of the THL model and the process of deriving transformation matrices and projection matrices of the THL model which were obtained from the previous work will be described in this section.

The THL model is the one in which the junction points of polymer networks are located at the points of a body-centered cubic lattice, and in which the arrangement of four strands projected from each junction point always takes the tetrahedral structure. The picture of the three dimensional structure of the THL model is given in Figure 1, where solid lines denote strands and small circles represent junction points. Here a word strand means a polymer chain which joins two neighboring junction points. A word junction point means the jointing part of strands in the networks.

In the THL model, it is assumed that the solute chain collections are regularly arranged at the lattice points, in turn with the solvent chain collections. For example, in Figure 1, A and C chain collections are composed of the sets of junction points of polymer solute molecules, and B and D chain collections consist of the sets of junction points of

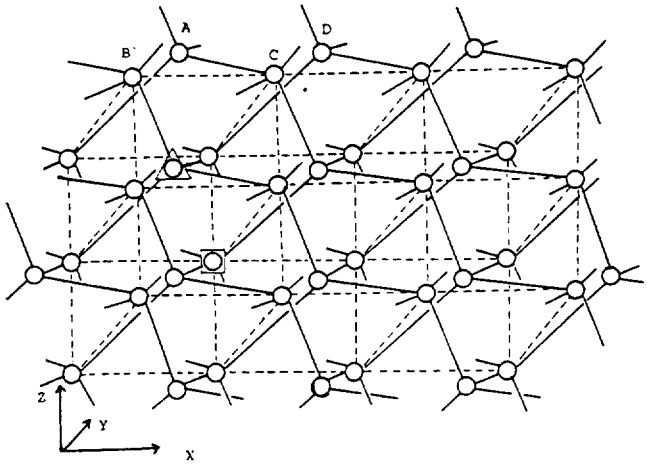

Figure 1. The three dimensional structure of the THL (tetrahedral lattice) model, where solid lines denote strands and small circles represent junction points. *A* and *C* chain collections are composed of the sets of junction points of polymer solute molecules, and *B* and *D* chain collections consist of the sets of junction points of polymer solvent molecules.

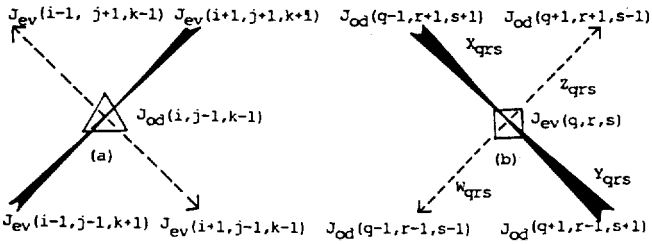

Figure 2. The characteristic combination modes of strands around the general junction points J_{oo} (a) and J_{ev} (b). This picture shows the spatial orientations of strands defined on the basis of a J_{ev}, in addition to the coordinates of junction points.

polymer solvent molecules. In each chain collection, junction points are classified into two categories according to the methods of their combination with neighboring strands. One is the set of junction points corresponding to the apexes of lattices, and the other to the body centers of lattices.

Let J_{ev}'s be junction points of the former and J_{oo}'s the latter. For either J_{ev}'s or J_{oo}'s, two different spatial orientations per junction point can be allocated in the way of combination with four neighboring strands around a given junction point. The effects of these two arrangements, however, are essentially identical in view of contribution to the free energy of the system, so it dosen't matter which of them is chosen in going on discussing. In usual, it is convenient to select a J_{ev} in the central part of the system as an origin of the coordinates.

Conveniently, if the length of an edge of lattices is taken as two without unit, the coordinates of every junction point can be readily described as the set of three components having only values of integers. The Figure 2 represent the characteristic combination modes of strands around the general junction points J_{ev}'s and J_{oo}'s and shows the spatial orientations of strands defined on the basis of a J_{ev}, in addition to the coordinates of junction points.

Independently of J_{ev} or J_{oo}, if l is taken as a position vector, the equations give its components and their areas as follows;

$$\begin{aligned} &l=(i,\ j,\ k)\\ &i=-I,\ -I+,\cdots,\ I-1,\ I\\ &j=-J,\ -J+1,\cdots,\ J-1,\ J\\ &k=-K,\ -K+1,\cdots,\ K-1,\ K \end{aligned} \tag{1}$$

where I, J, and K all take the values of positive integers. It is necessary to note that the components of every J_{ev} all have values of even integers, and that those of every J_{oo} have only values of odd integers. The spatial orientations of all the strands in the system are deduced to only four, as plotted in Figure 2(b). Conveniently, let σ_l or $\sigma_{i,j,k}$ ($\sigma=X$, Y, Z and W) be a symbol which represents a strand. Then the four spatial orientations of strands in the system are defined as

$$\begin{aligned} &X_{i,j,k}=\text{strand from } J_{ev}(i,j,k) \text{ to } J_{oo}(i-1,\ j+1,\ k+1)\\ &Y_{i,j,k}=\text{strand from } J_{ev}(i,j,k) \text{ to } J_{oo}(i+1,\ j-1,\ k+1)\\ &Z_{i,j,k}=\text{strand from } J_{ev}(i,j,k) \text{ to } J_{oo}(i+1,\ j+1,\ k-1)\\ &W_{i,j,k}=\text{strand from } J_{ev}(i,j,k) \text{ to } J_{oo}(i-1,\ j-1,\ k-1) \end{aligned} \tag{2}$$

The picture for these orientations is given in Figure 2(b). These are reduced to only four unit loops, that is, the twelve loops can be represented by the linear combination of four unit loops though the number of loops formed around a J_{ev} is all twelve. Similarly to the case of strands, let U_l or U_{ijk} ($U=\xi$, η, ζ, and δ) be the symbol denoting a loop. Then the four unit loops, which are all hexagonal types consisting of six strands, around a $J_{ev}(i,j,k)$ are expressed by

$$\begin{aligned} \xi_{ijk}&=X_{ijk}-W_{ij+2k+2}+Y_{ij+2k+2}-X_{i+2jk}+W_{i+2jk+2}-Y_{ijk}\\ \eta_{ijk}&=Y_{ijk}-X_{i+2j-2k}+Z_{i+2j-2k}-Y_{i+2jk-2}+X_{i+2jk-2}-Z_{ijk}\\ \zeta_{ijk}&=W_{ijk}-Y_{i-2jk-2}-Z_{i-2jk-2}-W_{ij+2k-2}+Y_{ij+2k-2}-Z_{ijk}\\ \delta_{ijk}&=X_{ijk}-Z_{i-2jk+2}+W_{i-2jk+2}-X_{i-2j-2k}+Z_{i-2j-2k}-W_{ijk} \end{aligned} \tag{3}$$

where the minus symbols attached to terms of the right-hand sides denote the inverse of orientation of the given strands.

The letters X, Y, Z, and W which are denoted along loops represent the orientation of strands defined by Eq. (2). In usual, it is convenient to discuss the physical properties of the system by separating J_{ev}'s and J_{oo}'s respectively in describing junction points of lattices. The formation mode of twelve hexagonal loops around any junction point is exactly identical for either a J_{ev} or a J_{oo} because the distinction of J_{oo}'s and J_{ev}'s derives only from the description of the coordinates.

The information obtained above can also be applied to the system of only J_{oo}'s after the consideration of the system composed of only J_{ev}'s. First, the system composed of only J_{ev}'s will be considered. Then it can readily be shown that the arranging structure of lattice in the system is that of the tetrahedral lattice.

Let i be the coordinate system of junction points, including all J_{ev}'s and J_{oo}'s, along the x-axis, then we have

$$\begin{aligned} &i=-I,\ I+1,\cdots,\ I-1,\ I\\ &I=2Q\\ &i'=-2Q,\ -2Q+2,\cdots,\ 2Q-2,\ 2Q \end{aligned}$$

$$q \equiv i'/2 = -Q,\ -Q+1, \cdots, Q-1,\ Q \tag{4}$$

where the quantities I and Q are positive integers, and in particular, I is a positive even integer. Similarly to the x-axis system, the following relationships along the axes y and z are given by

$$\begin{aligned} J &\equiv 2R \\ r &\equiv j'/2 \\ K &\equiv 2S \\ s &\equiv k'/2 \end{aligned} \tag{5}$$

where J and r correspond to the y-axis, and K and s correspond to the z-axis. Now if Eq. (3) is expressed by the newly reduced coordinate system (q, r, s), a series of equations can newly be obtained as the following;

$$\begin{aligned} \xi_{qrs} &= X_{qrs} - W_{qr+1s+1} + Y_{qr+1s+1} - X_{q+1rs+1} + W_{q+1rs+1} - Y_{qrs} \\ \eta_{qrs} &= Y_{qrs} - X_{q+1r-1s} + Z_{q+1r-1s} - Y_{q+1rs-1} + X_{q+1rs-1} - Z_{qrs} \\ \zeta_{qrs} &= W_{qrs} - Y_{q-1rs-1} + Z_{q-1rs-1} - W_{qr+1s-1} + Y_{qr+1s-1} - Z_{qrs} \\ \delta_{qrs} &= X_{qrs} - Z_{q-1rs+1} + W_{q-1r-1s} - X_{q-1r-1s} + Z_{q-1r-1s} - W_{qrs} \end{aligned} \tag{6}$$

where these equations are not arithmetic expressions, but symbolic ones, which will be transformed into arithmetic expressions later on. Especially, Eq. (6) is indispensable expressions in calculating the projection matrix $\Gamma^{\#}$ of the THL model. The unit loops around any J_{od} take the same linking form of strands as that of J_{ev}'s given in Eq. (5) because all the loops in the system are formed by exactly alternate linkings of J_{od}'s and J_{ev}'s.

Let J's be junction points, and σ's and U's represent strands and loops, respectively. And letting σ_L and U_L be all $(2L+1)$-dimensional row vectors, row vectors of strands and loops are given by

$$\begin{aligned} X_Q &= (X_Q X_{Q-1} \cdots X_{-Q+1} X_{-Q}) \\ X_R &= (X_R X_{R-1} \cdots X_{-R+1} X_{-R}) \\ &\cdots\cdots \\ \delta_R &= (\delta_R \delta_{R-1} \cdots \delta_{-R+1} \delta_{-R}) \\ \delta_S &= (\delta_S \delta_{S-1} \cdots \delta_{-S+1} \delta_{-S}) \end{aligned} \tag{7}$$

Let σ_{qrs} and U_{qrs} be defined as the form of triple products, that is,

$$\begin{aligned} \sigma_{qrs} &= \sigma_q \sigma_r \sigma_s \\ U_{qrs} &= U_q U_r U_s \end{aligned} \tag{8}$$

where though single terms of the right-hand sides have no physical meanings, triple product terms, each of which is composed of three single terms, have the same physical meanings as terms given in the left-hand sides. From Eqs. (7) and (8), σ and U take the form of row vectors expressed by

$$\begin{aligned} \sigma &= (X\ Y\ Z\ W) \\ U &= (\xi\ \eta\ \zeta\ \delta) \end{aligned} \tag{9}$$

where the X, Y, Z, $\cdots$, η, ξ, and δ are expressed by

$$\begin{aligned} X &= X_Q \otimes X_R \otimes X_S, & Y &= Y_Q \otimes Y_R \otimes Y_S \\ Z &= Z_Q \otimes Z_R \otimes Z_S, & W &= W_Q \otimes W_R \otimes W_S \\ \xi &= \xi_Q \otimes \xi_R \otimes \xi_R, & \eta &= \eta_Q \otimes \eta_R \otimes \eta_S \end{aligned}$$

$$\zeta = \zeta_Q \otimes \zeta_R \otimes \zeta_S, \qquad \delta = \delta_Q \otimes \delta_R \otimes \delta_S. \tag{10}$$

In Eq. (9), the symbol $\otimes$ represents a direct product between matrices. Let U_L be a $(2L+1)$-dimensional unit matrix given by

$$U_L = \begin{bmatrix} 1 & & & & \\ & 1 & & & \\ & & 1 & & \\ & & & \cdots & \\ & & & & 1 \\ & & & & & 1 \end{bmatrix} \tag{11}$$

and let D_L be a $(2L+1)$-dimensional matrix defined by

$$D_L = \begin{bmatrix} 1 & & & & & & 1 \\ -1 & 1 & & & & & \\ & -1 & 1 & & & & \\ & & -1 & 1 & & & \\ & & & \cdots & & & \\ & & & & -1 & 1 & \\ & & & & & -1 & 1 \end{bmatrix} \tag{12}$$

where all the blank parts in square brackets have the values of zeros, and such a usage will keep being used in the expressions of all the matrices appearing hereafter.

Let a, b, and c be matrices given by

$$\begin{aligned} a &\equiv U_Q \otimes D_R \otimes D_S \\ b &\equiv D_Q \otimes U_R \otimes D_S \\ c &\equiv D_Q \otimes D_R \otimes U_S \end{aligned} \tag{13}$$

where a, b, and c are al $[(2Q+1)(2R+1)(2S+1) \times (2Q+1)(2R+1)(2S+1)]$-dimensional matrices.

By use of Eqs. (11) to (13), Eq. (6) can be transformed from symbolic expressions into arithmetic ones, and then the results lead to

$$(\xi\ \eta\ \zeta\ \delta) = (X\ Y\ Z\ W) \begin{bmatrix} -b & -a & 0 & c \\ a & -b & c & 0 \\ 0 & -c & -b & -a \\ -c & 0 & -a & -b \end{bmatrix} \tag{14}$$

or

$$U = \sigma B \tag{15}$$

where B is defined by

$$B = \begin{bmatrix} -b & -a & 0 & c \\ a & -b & c & 0 \\ 0 & -c & -b & -a \\ -c & 0 & -a & -b \end{bmatrix} \tag{16}$$

From Eq. (14) or (15), it is shown that the matrix B, which has a $[4(2Q+1)(2R+1)(2S+1) \times 4(2Q+1)(2R+1)(2S+1)]$ dimension, is a transformation matrix transforming loops into a linear combination of strands.

Let C be defined by

$$C \equiv B \otimes B. \tag{17}$$

From the character of matrices,[12,15]

$$C^{\#} = B^{\#} \otimes B^{\#}. \tag{18}$$

The detailed contents for calculating $B^{\#}$ are shown in the previous works.[11~13] A number of elements of $B^{\#}$ for $Q=$

Table 1. The calculated values of the projection matrix B* on the THL model. These values are used in calculating the elastic energy of the given polymer system by using Eqs. (13) to (16). These are composed of the calculated values on the lattice system having the size that Q=R=S=20

(*q*, *r*, *s*)	(σ, σ')						
	(*X*, *X*)	(*X*, *Y*)	(*X*, *Z*)	(*X*, *W*)	(*Y*, *Z*)	(*Y*, *W*)	(*Z*, *W*)
(0, 0, 0)	−0.2713	−0.2713	0.2145	0.2043	−0.2614	0.2706	0.7312
(0, 0, 1)	0.5421	0.2374	−0.2914	0.5421	0.1043	−0.0498	0.5420
(0, 0, 2)	0.0971	0.0684	−0.0899	−0.0878	0.0432	0.0437	−0.0303
(0, 1, 14)	0.0943	−0.0876	0.0544	−0.0339	0.0291	−0.3327	0.0344
(0, 1, 19)	−0.0536	0.0440	0.0328	−0.0547	−0.0327	0.0294	0.0171
(0, 1, 20)	−0.0429	−0.0436	0.0872	0.0744	0.0443	0.0112	0.0096
(1, 0, 0)	0.3811	0.0584	0.3270	0.0429	−0.0374	0.0098	−0.0326
(1, 0, 1)	0.0862	−0.0322	−0.0341	0.0878	0.0099	−0.0081	0.0220
(1, 0, 2)	0.0666	0.0273	−0.0287	0.0534	0.0723	−0.0814	−0.0344
(2, 20, 0)	0.0098	0.0051	0.0096	−0.0523	0.0036	0.0058	0.0023
(2, 20, 1)	−0.0413	−0.0948	0.0390	−0.0054	0.0043	0.0394	0.0081
(2, 20, 2)	0.1143	0.1032	0.0946	0.0222	−0.0062	−0.0073	−0.0039
(10, 10, 10)	0.0093	0.0088	−0.0077	0.0049	0.0057	−0.0033	0.0091
(20, 19, 18)	0.0042	0.0037	0.0032	−0.0032	0.0033	0.0032	0.0043
(20, 19, 19)	0.0919	0.0927	−0.0934	−0.0217	0.0324	−0.0994	0.0059
(20, 19, 20)	0.1114	−0.0981	0.0226	0.0243	−0.0814	0.0343	0.0274
(20, 20, 18)	−0.3689	0.1123	−0.0094	0.2023	−0.0913	0.0814	0.0625
(20, 20, 19)	−0.0824	0.0243	0.0048	0.0382	0.0375	0.0586	−0.0417
(20, 20, 20)	0.0332	0.2716	0.3571	−0.1982	0.5044	0.5273	−0.0394

$R=S=20$ are given in Table 1. In Table 1, since the strand pairs (*X*, *X*), (*Y*, *Y*), (*Z*, *Z*), and (*W*, *W*) all have the same values, they can be represented only as the (*X*, *X*). On the other hand, (*X*, *Y*) has the same value as (*Y*, *X*); (*X*, *Z*) as (*Z*, *X*); (*X*, *W*) as (*W*, *X*); ···; and (*Z*, *W*) as (*W*, *Z*).

In the result, totally seven of independent paris (σ, σ')'s for any junction point are obtained. In order to obtain Γ^* by using the first equation of Eq. (A7) of appendices, we have only to find C^*. Since any element of C^* is given by direct products of two of B^*'s, if Γ^* $[(\sigma_{qrs}, \sigma'_{q'r's'})$ $(\sigma''_{q''r''s''}, \sigma'''_{q'''r'''s'''})]$ is set to be an element of the matrix Γ^* for the pairs $(\sigma_{qrs}, \sigma'_{q'r's'})$ and $(\sigma''_{q''r''s''}, \sigma'''_{q'''r'''s'''})$, the following equation can be obtained;

$$\Gamma^*[(\sigma_{qrs}, \sigma'_{q'r's'})(\sigma''_{q''r''s''}, \sigma'''_{q'''r'''s'''})] = B^*(\sigma_{000}, \sigma'_{|q'-q_{q''}-r_{q''}s'-s_{s''}|}) \cdot B^*(\sigma''_{000}, \sigma'''_{|q'''-q'_{q''}+r'_{q''}s'''-s''_{s''}|}) \quad (19)$$

from which all the other elements of Γ^* are obtained. Having calculated the projection matrix Γ^* of the THL model, F_2 can be obtained from Eqs. (19) and (A16) of appendices.

The important skeleton of topological theories is transformation matrices, distribution functions, and free energy about polymer systems. The concept and the deriving process of all these items are briefly given in appendices. In topological theories, the total free energy of polymer networks consists of four energy terms (see Eq. (A3) of appendices). The topological free energy, $F_{o,top}$ (which is free energy arising from the topological interaction among the strands), can be obtained from the values of contact distribution functions (*e.g.*, g_p and h_p). The calculation of projection matrices of the THL model must be carried out before obtaining the strand fluctuation energy, F_2 (which is free energy from the fluctuation of strands). Therefore, the transformation matrix (from which a projection matrix can be obtained) of Eq. (16) had been offered in the previous work.[13] In the present work, the calculation of free energy of several polymer blends[16,20~23] has been carried out by using the given matrices. Thus, the total free energy of the network can completely be computed through the process discussed up to now.

Topological Analysis of the Tsenoglou's Theory

The Tsenoglou's theory[14] is mainly referred to entanglement statistics in miscible polymer systems. It is assumed that the linear flexible polymers of sufficiently large molecular weight form a temporary network of entangled chains in dense solutions or melts. The molecular weight between entanglements, M_e, increases with the molecular rigidity of the polymer and with solvent concentration. In general, it is expected that entanglements between identical chains lie further apart in a blend than in a pure system, and entanglements associating heterogeneous polymers are formed in the areas between homopolymer junctions.

For a blend composed of m different polymer species, let M_i, V_i, and ρ_i $(i=1,2,\cdots,m)$ be the molecular weight, the volume fraction, and the density of the ith component, respectively. Let M_{ie} be the molecular weight between entanglements, and let N_{ie} be the number of primitive steps (*i.e.*, subsegments defined by two consecutive chain junctions) per chain, then the following relationship is obtained by

$$N_{ie}=M_i/M_{ie}-1$$

$$\simeq M_i/M_{eio} \tag{20}$$

Let ij be defined as a segment which is lying on an i polymer chain and confined by two successive entanglements with j polymers, N_{ij} as the number of such segments per i chain, and M_{eij} as its average molecular weight.

When the end effects are neglected ($N_i \gg 1$), the total number of steps per blended i chain (n_i) is given by

$$N_i = \sum_{j=1}^{m} N_{ij} = \sum_{j=1}^{m} (M_i/M_{eij}) - 1 \simeq \sum_{j=1}^{m} (M_i/M_{eij}) \tag{21}$$

It is assumed that the fraction of entanglements along an i chain caused by associations with j chains is equal to the fractional participation of j steps in the total step population in the blend if perfect randomness prevails in the formation of interchain couplings. The number density of steps of any kind is given by

$$S = \sum_{j=1}^{m} \nu_j N_j \tag{22}$$

where ν_j represents the number of j chains per unit volume of the blend, and its detailed form is given by

$$\nu_j = \rho_j v_j N_A / M_j \tag{23}$$

where N_A is the Avogadro's number.

In usual, the entanglement probability between dissimilar chains is proportional to the geometric average of those between similar chains. Unless compatible neighbors affect the ability of similar polymers to entangle, the frequency of associations between chains of the same species decreases with the polymer volume fraction. Thus, the molecular weight between two successive homopolymer entanglements along a third chain can be computed as a function of the blend composition and the corresponding properties of the pure polymeric precursors;

$$M_{eij} = \frac{M_i}{N_{ij}} = \frac{1}{V_j}\left(\frac{M_{eio}M_{ejo}}{r_j/r_i}\right)^{1/2} \tag{24}$$

And also the total number of primitive steps along an i chain, N_i, is given by

$$N_i = \frac{M_i}{M_{eio}} \sum_{j=1}^{m} V_j \left(\frac{\rho_j M_{eio}}{\rho_i M_{ejo}}\right)^{1/2} \tag{25}$$

It is assumed that the above relationship is valid even in the case that some of the blend components are oligomers or regular solvents. The inability of the small molecules to form entanglements can be explained by setting their value of M_{eo} to approach to infinity.

By the way, the polymer mixing affects the ability of blended polymers to entangle.[16] Describing this phenomenon quantitatively, the following equation is given by

$$\frac{M_{eii}}{M_{ei}} = \frac{N_{ii}}{N_{io}} = V_i\left(1 + \sum_{\substack{j=1 \\ i \neq j}}^{m} \in_{ij} \frac{N_{ij}}{N_{ii}}\right)^{\pm 1} \tag{26}$$

The positive or negative exponent in Eq. (26) represents attractive or repulsive interactions between dissimilar species, and such a usage will keep being used hereafter. The parameter $\in_{ij}$ represents the relative strength of these interactions. Its positive value corresponds to the fractional change (decrease or increase) of the distance between two successive homopolymer entanglements along an i chain due to the intermediate presence of a single entanglement with a dissimilar (j) species.

Usually, it is expected that the change of N_{ij} is proportional to that of N_{ii} and that the ratio N_{ij}/N_{ii} remains relatively insensitive to $\in$ variations. Thus, from Eqs. (24) to (26), the following equation can be obtained by

$$\frac{M_{eio}}{M_{ei}} = \frac{N_{ii}}{N_{io}} \simeq V_i\left[1 + \sum_{\substack{j=1 \\ i \neq j}}^{m} \in_{ij}\left(\frac{V_j^2 \rho_i M_{eio}}{V_i^2 \rho_i M_{ejo}}\right)^{1/2}\right]^{\pm 1} \tag{27}$$

Combination of Eq. (27) with Eqs. (20) and (23) leads to

$$\frac{1}{M_{eij}} = \frac{N_{ii}}{M_i} = \frac{V_i}{M_{eio}}\left[1 + \in\left(\frac{V_j^2 \rho_j M_{eio}}{V_i^2 \rho_i M_{ejo}}\right)^{1/2}\right]^{\pm 1} \tag{28a}$$

$$\frac{1}{M_{eij}} = \frac{N_{ij}}{M_i} = V_j\left(\frac{\rho_j/\rho_i}{M_{eio}M_{ejo}}\right)^{1/2}\left[\left(1 + \in\left(\frac{V_i^2 \rho_j M_{eio}}{V_j^2 \rho_i M_{ejo}}\right)^{1/2}\right)\left(1 + \in\left(\frac{V_i^2 \rho_j M_{ejo}}{V_j^2 \rho_i M_{eio}}\right)^{1/2}\right)\right]^{\pm 1/2} \tag{28b}$$

For the topological THL model, let the parameter $\in$ be represented by

$$\in = \alpha \Psi P \tag{29}$$

where α is a normalized constant, Ψ is the solute-solvent distribution function [see Eq. (A8)], and P is the chain contact distribution function considering excluded-volume effects in the given blend. Introduction of Eq. (29) enables the Tsenoglou's theory to be transformed into a topological theory, and Eq. (29) is first and originally offered in the present work. Also an offer of Eq. (29) is one of the most important parts of the work which has been carried out in this paper. The detailed form of P is respectively given by

$$P = \xi(3\nu'^2/2\pi l^2 u\ \bar{u}\ v\ \bar{v}\ k_1)^{3/2} \cdot \exp\{-3(k_3 - k_2^2/k_1)/2l^2\} + (1-\xi)\{9\nu'^2/4\pi^4\ l^4 \cdot \bar{u}\ \bar{v}\ u'\ v'\ \Delta u\ \Delta v_{\|k_1\|}]^{3/2} \times \exp\{-3(k_3 - k_2 k_1^{-1} k_2)2l^2\} \tag{30}$$

where ξ is the distribution probability parameter, which has the variation values less than one and more than zero, and all the physical meanings of the others are represented by the previous references.[11-13]

Combination of Eq. (29) with Eqs. (28a) and (28b) leads to

$$M_{eii} = \frac{M_{eio}}{V_i}\left(1 + \alpha \Psi P\left\{\frac{V_i^2 \rho_i M_{eio}}{V_i^2 \rho_i M_{ejo}}\right\}^{1/2}\right)^{\mp 1} \tag{31a}$$

$$M_{eij} = \frac{1}{V_j}\left\{\frac{M_{eio}M_{ejo}}{\rho_j/\rho_i}\right\}^{1/2}\left[\left\{1 + \alpha \Psi p\left(\frac{V_i^2 \rho_j M_{eio}}{V_i^2 \rho_i M_{ejo}}\right)^{1/2}\right\}\left\{1 + \alpha \Psi P\left(\frac{V_i^2 \rho_i M_{eio}}{V_j^2 \rho_j M_{eio}}\right)^{1/2}\right\}\right]^{\mp 1} \tag{31b}$$

Multicomponent Polymer Systems. Now consider network elasticity in multicomponent polymer systems. Let G_N° be the viscoelastic parameter representing a measure of the material rigidity of entangled polymer solutions and melts. For a pure polymeric fluid i, let G_{Ni}° be the pseudo

equilibrium shear modulus of the temporary network formed by the free chains. Then its magnitude is inversely proportional to the mesh size of this network such as

$$G^{\circ}_{Ni}=k_BT\nu_i N_i\ RT\ \rho_i/M_{eio} \tag{32}$$

where T is the temperature, k_B is the Boltzmann constant, and R is the ideal gas constant. The plateau modulus of a multicomponent macromolecular blend G°_{NB} can be obtained by

$$G^{\circ}_{NB}=k_BT\sum_{i=1}^{m}\nu_i N_i=k_BT\Big(\sum_{i=1}^{m}(\nu_i N_{ii})^{1/2}\Big)^2 \tag{33}$$

Considering the effects of thermodynamic interactions, the rubbery plateau modulus of a binary miscible is given by

$$(G^{\circ}_{NB}{}^{\circ})^{1/2}=V_1(G^{\circ}_{N1})^{1/2}(1+\alpha\Psi P\{V_2(G^{\circ}_{N2})^{1/2}/V_1(G^{\circ}_{N1})^{1/2}\})^{\pm 1/2}+V_2(G^{\circ}_{N2})^{1/2}(1+\alpha\Psi P\{V_1(G^{\circ}_{N1})^{1/2}/V_2(G^{\circ}_{N2})^{1/2}\})^{\pm 1/2} \tag{34}$$

where the positive or negative exponent represents mutually attractive or repulsive components. The result of Eq. (34) can be normalized by

$$Y=\frac{(G^{\circ}_{NB})^{1/2}-(G^{\circ}_{NB})^{1/2}}{(G^{\circ}_{N1})^{1/2}-(G^{\circ}_{N2})^{1/2}} \tag{35}$$

where all the values with the variation of the blend composition are subjected to a unified plot.

Interpenetrating Polymer Networks (IPN). It is now the time to consider equilibrium modulus of interpenetrating polymer networks. Unless the presence of permanent junctions affects the entanglement density, such analysis as the case of free polymer chains in a fluid can also be applied to an interpenetrating polymer network (abbreviated to IPN hereafter) composed of m interlocked rubber networks. In the case of the ith component of this system ($i=1,2,\cdots$, m), let M_i be the average molecular weight of a crosslinked strand, let $\rho_i V_i$ be the concentration, and let M_{eio} be the molecular weight between entanglements without any other component ($V_i=1$).

A strand in the ith network consists of N_i+1 steps, and N_i steps are formed by entanglements trapped during the crosslinking process. In usual, one step is due to the crosslinks at the end of the chain.

Since the mobility of the free end is confined, all the steps which are lying on or terminated by a tethered segment are elastically ineffective.[17~18]

Letting $1-\phi_i$ be the fraction of the dangling ends in the ith network, the number density of the elastically active i strands, ν_{ei}, is given as follows;

$$\nu_{ei}=\phi_i\nu_i \tag{36}$$

Though each of these strands is still composed of N_i+1 steps, only $N_{ei}+1$ of them can store energy under deformation. In order to calculate this number, and to account for the network weakening due to the chain defects, the following relationship may be used by

$$1+N_{ei}=1+\frac{M_i}{M_{ej}}\sum_{j=1}^{m}\phi_j V_j\Big(\frac{\rho_j M_{eio}}{\rho_i M_{ejo}}\Big)^{1/2} \tag{37}$$

For a randomly crosslinked network, the following relation is given as shown first by Flory;[17]

$$1-\phi_i=1/C_i \tag{38}$$

where C_i is the number of tetrafunctional crosslinks per primary i chain.

Applying the statistical theory of rubber elasticity into the IPN systems, the equilibrium shear modulus G_e is proportional to the concentration of elastically active segments ν_e;

$$G_e=Ak_BT\nu_e \tag{39}$$

where the quantity A, which is close to unity, is a factor which explains the effects of the junction mobility and the reduction of the chain dimensions caused by crosslinking. Besides strands formed by crosslinking are the factors of material rigidity, the subsegments (steps) formed by entanglements trapped between permanent junctions can also store elastic energy, and then contribute to ν_e such as;

$$A\ \nu_e=\sum_{i=1}^{m}A_i\nu_{ei}(1+N_{ei}) \tag{40}$$

For an athermal system formed by m IPN's which contain dangling branches, combination of Eqs. (39) and (40) with Eqs. (36), (37), and (23) leads to

$$\frac{G_e}{RT}=\sum_{i=1}^{m}\phi_i V_i\Big(\frac{\rho_i}{M_i}\Big)+\Big[\sum_{i=1}^{m}\phi_i V_i\Big(\frac{\rho_i}{M_{eio}}\Big)^{1/2}\Big]^2$$

or

$$G_e=\sum_{i=1}^{m}\phi_i V_i G_{ci}+\Big[\sum_{i=1}^{m}\phi_i V_i(G^{\circ}_{Ni})^{1/2}\Big]^2 \tag{41}$$

where $G_{ci}=RT\rho_i/M_i$ is regarded as the measure of the crosslink contribution to the material rigidity.

For the case where $m=1$ and $V_i=1$, Eq. (41) reduces to Ferry's equation for the modulus of a one-component network with trapped entanglements;[18]

$$G_{ci}=RT\ \phi_i\rho_i(1/M_i+\phi_i/M_{eio}) \tag{42}$$

Using the same method and considering the effects of thermodynamic interactions, the modulus of a binary IPN is given by

$$G_e=(\phi_1V_1G_{c1}+\phi_2V_2G_{c2})+(\phi_1V_1(G_{12})^{1/2}+\phi_2V_2(G_{21})^{1/2})^2 \tag{43a}$$

where

$$G_{ij}=G^{\circ}_{Nj}(1+\alpha\Psi P\{\phi_jV_j(G^{\circ}_{Nj})^{1/2}/\phi_iV_i(G^{\circ}_{Ni})^{1/2}\})^{\pm 1} \tag{43b}$$

It is necessary to recall that the positive or negative exponent in Eq. (43b) represents attractive or repulsive interactions between dissimilar species. For a binary IPN where the first participating network is isotropically swollen by the second, the form of Eq. (43a) is reformed into

$$G_e=\phi_1V_1{}^{1/3}G_{c1}+\phi_2V_2G_{c2}+\phi_1{}^2V_1{}^{4/3}G_{12}+\phi_2{}^2V_2{}^2G_{21}+(V_1{}^{1/3}V_2+V_1V_2)\phi_1\phi_2(G_{12}G_{21}) \tag{44}$$

Accommodating the network strengthening effects of trapped entanglements, Eq. (44) results in an extension of an earlier result reported by Sperling.[19]

Results and Discussion

The results of the Tsenoglou's theory are analyzed in view

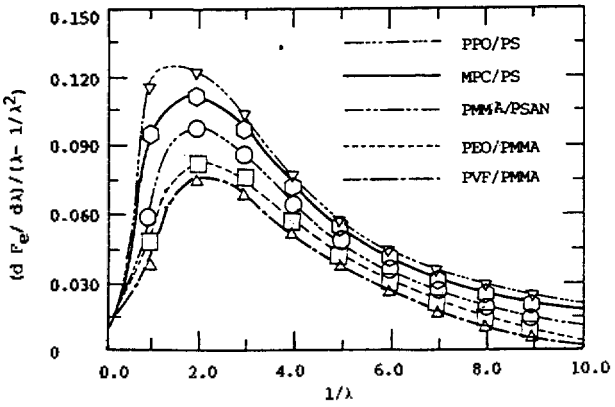

Figure 3. The calculated values of elastic free energy obtained by applying Eqs. (A13) to (A16) to the given polymer blends (*e.g.*, PPO/PS, MPC/PS, PMMA/PSAN, PEO/PMMA, and PVF/PMMA). The experimental data points (which are represented as polygons and circles) converted from the Refs.[16,20-23] are plotted in this picture.

of topological theories, so that various equations of the Tsenoglou's theory are transformed into those expressed by parameters of topological theories. The degree of participation of solvents into the solute-solvent system which constitutes polymer blend systems affects the distribution states of elastic free energy between the whole entangled chains. The free energy of polymer blend systems is directly affected by the distribution functions according to the contribution extent of the solvent and solute skeleton. The distribution functions of these solvents have the forms of distribution function equations obtained by the previous topological theories,[13] the contribution terms of solute are the values determined dependently if the distribution function of solvent has only to be determined.

The determination of distribution functions about these solvent-solute systems can be carried out by the calculation of the projection matrices of corresponding lattice systems (*e.g.*, the THL model), and the calculation of projection matrices takes different values depending on the degree of contribution of the term of solvent. For the system in which the contribution of the solvent term leads to 0.05%, the calculation value of the typical projection matrix $\Gamma^{\#}$ is given in Table 1. As shown earlier, the total elastic free energy of the polymer system is composed of $F_{o,ph}$, $F_{o,top}$, F_1, and F_2 (see Eq. (A4) of appendices).

The length of strands of each component polymer which moves about in polymer blends affects single and double contact probabilities (*e.g.*, g_p and h_p) between strands. Usually, the longer the length of strands is, the greater the values of single and double contact probabilities of strands are. The greater the values of these distribution functions are, the greater the values of contribution terms of free energy are, and the larger the values of total free energies are in polymer blend systems. Such an aspect is shown in Figure 3.

The values of curves of free energy have been calculated by using Eqs. (A13) and (A16), and then plotted in Figure 3. Also the experimental data converted from the Refs. 16, 20-23 are plotted in Figure 3. The various polygons (*e.g.*, inverse triangles, hexagons, circles, squares, and regular tri-

Table 2. The values of parameters used in calculating the elastic energy curves on the given polymer blends

Parameter / blend system	δ (×10)	ξ (×10)	α (×10⁴)	ρ (×10³)
PPO/PS	3.242	7.543	3.784	9.483
MPC/PS	4.437	8.764	3.958	8.441
PMMA/PSAN	2.146	8.911	4.013	8.379
PEO/PMMA	5.381	8.953	4.162	8.145
PVF/PMMA	7.477	8.969	4.287	8.027

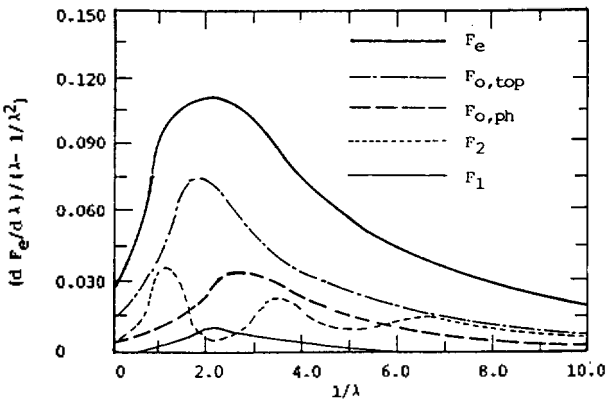

Figure 4. The curves related with $F_{o,ph}$, $F_{o,top}$, F_1, and F_2 for the polystyrene blend system (MPC/PS).

angles) which are located intermittently along the calculated curve of each sample represent experimental data points converted from the given references. Here it is proved that the theoretical results show good agreemeent with the given experimental data. The polymer blends plotted in Figure 3 are PPO(poly-(2,6-dimethylphenyleneoxide))/PS(polystyrene),[20] MPC(tetramethylpolycarbonate)/PS,[21] PMMA(poly(methylmethacrylate))/PSAN(poly(styrene-acrylonitrile)),[22] PEO(poly(ethyleneoxide))/PMMA,[23] PVF(poly(vinylidene fluoride))/PMMA[16] blend systems.

The parametric values about each sample, used in calculating these theoretical values, are shown in Table 2. Concretely speaking, such are δ, ξ, α, and ρ. The quantity ξ is the distribution probability parameter, which has the variation values less than one and more than zero (see Eq. (30)). α is a normalized constant (see Eq. (29)). ρ is the number density parameter of j chains per unit volume of the blend (see Eq. (23)). The physical meaning of δ is the ratio of the end-to-end distance of a strand in the standard configuration versus that of a strand in the phantom network.

The curves related with $F_{o,ph}$, $F_{o,top}$, F_1, and F_2 for the polystyrene system are plotted in Figure 4. In Figure 4, the graphs of the total free energy and each component energy of the MPC/PS blends are plotted in the shapes of curves. As shown in Figure 4, $F_{o,top}$ is the first, and $F_{o,ph}$ is the second in order of contribution to the total free energy. Usually, $F_{o,ph}$ is treated with the functions of distance of displacement between junction points. Though the contribution of F_2 and F_1 is a little, these energy terms contribute to the total free energy in a regular pattern. It is regarded that such a contri-

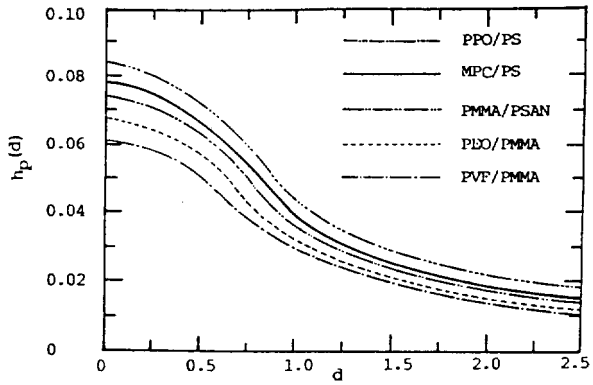

Figure 5. The calculated curves of $h_p(d)$'s as functions of d, which is a distance between the centers of the strands. These values are used in calculating $F_{o,top}$.

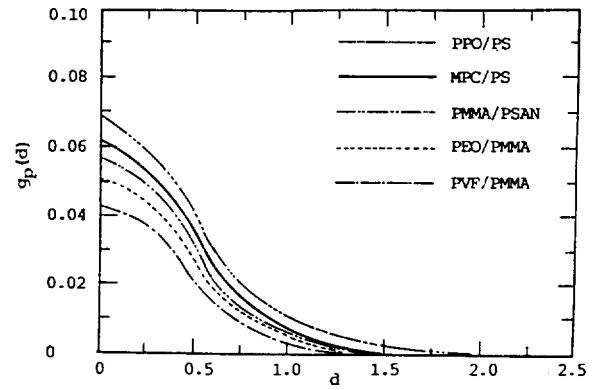

Figure 6. The calculated curves of $g_p(d)$'s as functions of d, which is a distance between the centers of the strands. These values are used in calculation $F_{o,top}$.

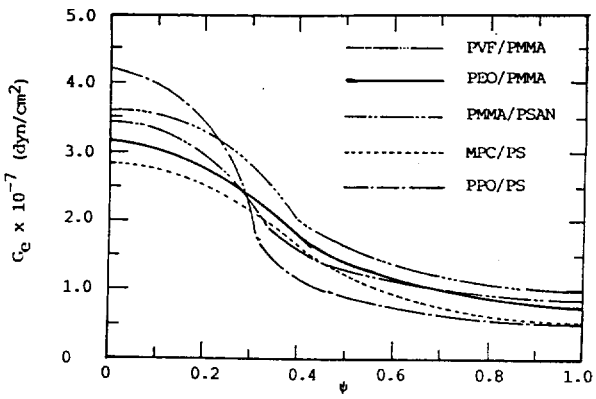

Figure 7. The calculated curves of G_e evaluated from Eq. (43) versus ψ.

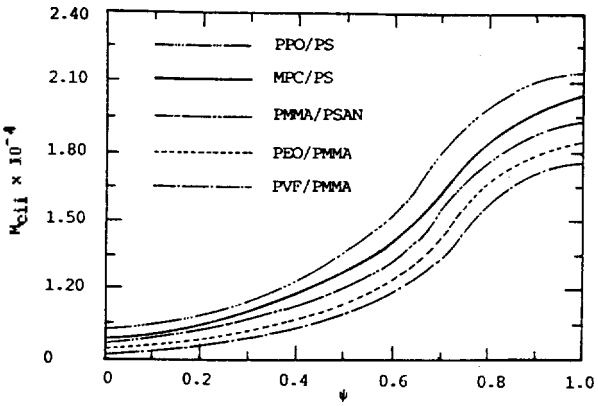

Figure 8. The calculated curves of M_{ii} evaluated from Eq. (31a) versus ψ.

bution pattern of each component energy term to the total free energy is alike to those of other polymer blend systems.

In order to evaluate $F_{o,top}$ for each blend system, the values of distribution functions h_p and g_p should be calculated. A series of h_p and g_p functions are given in Figure 5 and in Figure 6, respectively. Figure 5 is the graph which plots the double contact distribution function displacement of centers of strands for a strand having constant length. It is shown that the larger the length of strands is, the greater the vlaues of distribution functions are. Here we see that the values of distribution functions of polymer blends are exactly arranged with order of total free energy values of the given polymer blends. In other words, the order of distribution functions of Figure 5 is exactly alike to order of total free energies of Figure 3.

Figure 6 is the graph which plots the single contact distribution function displacement of centers of strands for a strand having constant length. The pattern of Figure 6 resembles that of Figure 5, but all of the values of functions are smaller than the values of functions of Figure 5. Such a phenomenon is self-evident in that the probability of double contact is greater than the probability of single contact. It is shown that the order of values of distribution functions of Figure 6 is exactly alike to the one of Figure 5.

The related graphs of G_e versus Ψ evaluated from Eq. (43), are given in Figure 7. Also the relationship with the experimental data obtained from the previous reference is shown in Figure 7. Figure 7 represents the curves of equilibrium shear moduli G_e's of several polymer blends, which are plotted with the values of the solute-solvent distribution functions (see Eq. (43)). The merit of the present work is the fact that for the Tsenoglou's work, the values of G_e's of only the confined areas of the solute-solvent distribution can be offered, while for the present work, all the values of G_e's of the full areas of the solute-solvent distribution can be offered.

The values of G_e's change greatly around the Ψ value of about 0.3. Such a phenomenon is basically caused by the fact that for the PVF/PMMA and PMMA/PSAN blends, the effect of topological interaction due to miscibility of heterogeneous polymer strands gets larger.

The relationship with M_{ii} versus Ψ is shown in Figure 8, and the relationship with M_{ij} versus Ψ is given in Figure 9. Figure 8 is the graph which plots the values of average molecular weight of homogeneous polymer strands of five polymer blend systems according to the changing values of the solute-solvent distribution function. As shown previously, the order of decrement of length of strands of polymer blends is arranged as follows; PPO/PS, MPC/PS, PMMA/PSAN, PEO/PMMA, and PVF/PMMA.

Figure 9 is the graph which plots the values of average

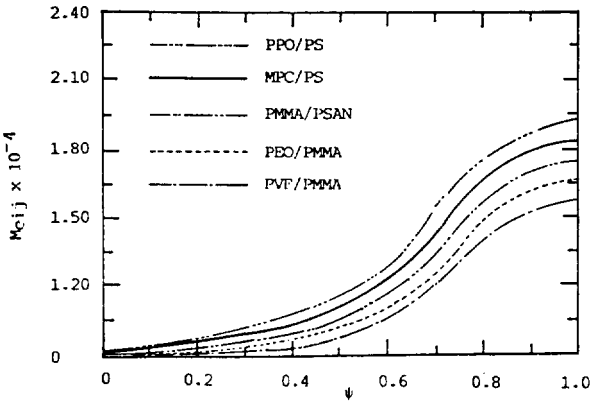

Figure 9. The calculated curves of M_{ej} evaluated from Eq. (32b) versus ψ.

molecular weight of heterogeneous polymer strands of the five polymer blend systems according to the changing values of the solute-solvent distribution function. The order of values of molecular weight is exactly the same as that of Figure 8. Generally, the greater the values of molecular weight of strands are, the greater the interaction between strands is.

In the case of lattice systems necessary in calculating projection matrices, the values of Q, R, and S used in Eqs. (4) and (5) are equally twenty. It is proved that the size of the lattice system of such an extent is sufficient in describing the physical meanings of polymer blend systems.

Letting v be the degree of polymerization, such polymers as polyisoprene, polystyrene, and poly(dimethyl siloxane) have the values[12] of about 30 to 300. It is assumed that the whole systems of the blends considered here are composed of the THL's. For the THL model, a cell has 128 junction points and 256 strands.[13]

It is necessary to consider the relationship between cells and the whole lattice system. Let l, m, and p be the sets of the coordinates of integers along the axes x, y, and z, respectively. Then we have

$$\begin{aligned} l &= -8L,\ -8L+1,\cdots,\ -1,\ 0,\ 1,\cdots,\ 8L-2,\ 8L-1 \\ m &= -8M,\ -8M+1,\cdots,\ -1,\ 0,\ 1,\cdots,\ 8M-2,\ 8M-1 \\ p &= -8P,\ -8P+1,\cdots,\ -1,\ 0,\ 1,\cdots,\ 8P-2,\ 8P-1 \end{aligned} \quad (45)$$

where L, M, and P are all positive integers.

As referred to previously, a strand represents a polymer chain which is fixed at any two of junction points. The degree of polymerization, v, have the values of about 30 to 300 for such polymers as polyisoprene, polystyrene, and etc.[12] It is assumed that the whole systems of polymer blends considered here are composed of the THL's. A cell is composed of eight subcells. A cell has one hundred and twenty eight junction points and two hundred and fifty six strands.

In the lattice model, the standard configuration represents the form of arrangement in which all the strands are arranged linearly with all the strands pressed tightly in the form of springs. In the case of calculation of projection matrices, the standard configuration of lattices has often been taken as the reference state of the system.

The definition of δ is given by the ratio of the end-to-end distance of a strand in the standard configuration versus that of a strand in the phantom network, that is,

$$\delta = 3^{1/2} d_o / (v^{1/2}\ b) \quad (46)$$

where d_o is a half of the length of an edge of the lattice, v is the degree of polymerization, and b is the length of a segment. Typical elastic polymers, such as polyisoprene, polystyrene, and etc. whose v values are given as 30 to 300, have the δ values of 0.2 to 0.8.

The curves of the total free energy and each component energy is plotted in Figure 10 for the PVF/PMMA blend. We see that the pattern of the contribution of each component energy to the total free energy is similar to that of Figure 3.

Conclusion

The gist of the present work is the work that first transforms the parameter ∈ of the Tsenoglou's theory into the form of $\alpha P\Psi$ of topological theories, and obtains the curves of the total free energy of polymer blends against the values of inverse strain, then calculates theoretically the values of equilibrium shear moduli and molucular weight of polymer blend systems according to the changing values of the solute-solvent distribution function by assuming the five given polymer blend systems as the THL model. The central content is the fact that the interaction between strands of polymer networks mainly contributes to the total free energy of polymer systems. It is known that the contributive part due to displacement of junction points is smaller than that of strands.

Especially, the excellent merit of the present work is located in the fact that the previous Tsenoglou's work can obtain corresponding physical properties only for polymer blends having confined compositive ratios, while the present work can calculate and obtain corresponding physical properties (*e.g.*, molecular weight, equilibrium shear moduli, and total free energy) over all the solute-solvent distribution as possible as can be (see Figures 7-9).

In order to analyze topologically the Tsenoglou's theories, the values of molecular weights and moduli are represented with topological theories by establishing the THL model. Especially, the parameter ∈ has been analyzed with the combination functions of the wave functions of topological theories, and transformed into the types of functions obtained from the results of projection matrices.

According to topological theories, the free energy of the blend system contains the elastic energy caused by contact of strands as the mainly contributive parts. For polymer blend systems, the distance of the junction points which have cross-link each other is changed depending on the state of distribution of solute-solvent. In order to discuss such an aspect strictly, it is necessary to treat systematically interaction between strands which form the lattice structure by assuming the five given polymer blend systems as the THL model. It is assumed that all the miscible polymer blends form the lattice structure of the THL model whether the state of polymer blends is solid or not. It is regarded that such an assumption is reasonable when considering the motion of polymers for a constant average time interval.

The average length of strands can be obtained from the values of molecular weight of corresponding polymers. The vlaues of single and double contact distribution functions

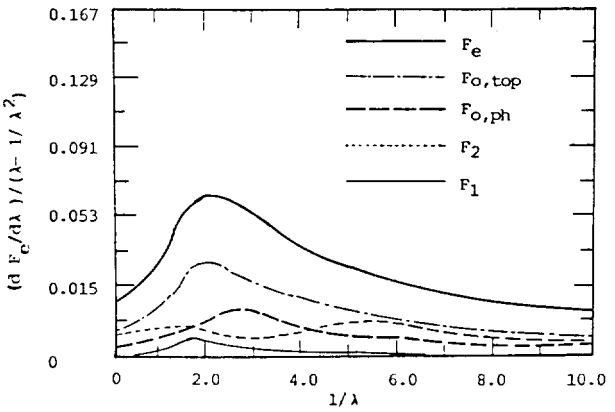

Figure 10. The component curves of free energy on the polymer blend PVF/PMMA. these calculated curves are obtained by applying Eqs. (A13) to (A16) to the given polymer system.

can be calculated from information about the length of strands. Actually, these values of contact distribution functions afford the detailed scale of interaction by entanglement of strands.

Once the values of these contact probability functions are known, the value of interaction energy by entanglement between strands can be obtained. And also once the values of projection matrices are known, the contribution of free energy by fluctuation of junction points can be obtained. In this way, the values of the total free energy have been obtained, as functions inverse strain, from contact distribution functions and projection matrices for all the given polymer blends.

In Figure 10, the graphs of each component of elastic energy are plotted. The graphs of curves of free energy depending upon $1/\lambda$ for PVF/PMMA are shown in Figure 10, where the curves are represented with the values of the parameter δ in Figure 10. Since the contact probabilities of strands are increased with increment of the degree of polymerization ν, the more the degree of polymerization is decreased, the more the value of δ is increased, and then the more the contribution to F is increased. The peaks of curves of energy move towards the left side of the x axis.

The cause of such a phenomenon may be originated from the fact that the interaction between strands is sensitively affected by the values before or behind one because of the increment of ν.

For each polymer blend, according to the degree of contribution of the solvent participated, there are variously changed the values of contact distribution functions among solvent-solute, solute-solute, and solvent-solute molecules. These patterns ar shown in Figures 5 and 6.

The greater the values of functions of single or double contact are, the more the contribution to elastic free energy is increased.

For the blends considered here, the fact has been testified that the order of the systems in which topological interaction is great is arranged as follows; such are PPO/PS, MPC/PS, PMMA/PSAN, PEO/PMMA, and PVF/PMMA. And it is shown that the total free energy in polymer networks gets greater in the same order as the case of length of strands. As discussed so far, the values of length of strands differ depending upon the distribution state of solute-solvent, such a result affects the values of molecular weight and shear moduli in a constnat pattern. The longer the length of strands is, the greater the contribution part of free energy caused by topological interaction is, and resultantly the larger the values of the total free energy are. Such an aspect has been shown even in the values of molecular weight and moduli which were offered in the previous Tsenoglou's work. Alternatively speaking, the present work has good agreement with the previous Tsenoglou's work.

The effects of interaction of strands by entanglement affect distribution functions among strands, these affect each value of projection matrices produced from the THL model, and then ultimately affect elastic energy originated from topological interaction. The evaluated values of parameters are given in Table 2. Each value of these affords detailed information in relation to the phenomena of topological entanglement of each blend.

In the while, the curves related to equilibrium shear moduli and distribution function ψ are given in Figure 7, where it is exposed that the more greater the values of distribution functions are, the more increased the values of plateau moduli are. As the cause of such a inclination, it is regarded that the degree of entanglement among chains directly contributes to the values of plateau moduli in the case of the polymer blends composed of solute-solvent systems.

The degree of variation of molecular weights among steps is shown in Figures 8 and 9 with the values changing regularly.

In the case of each polymer blend considered here, the graphs of the result of topological management are shown in Figure 3. The experimental values reduced from the Refs. 16, 20-23 are also given in Figure 3. As shown in the graphs, it is exposed that the theoretically calculated values are good agreement with the experimental data reduced from the references.

As discussed so far, we see that the physical quantities, treated with only as simple parameters previously, of the Tsenoglou's theories have the close relation with contact functions and distribution functions contributed to entanglement. As shwon previously, judging from good agreement of topological results with experimental data, it can be regarded as logical and reasonable that the parameter $\in$ has been transformed into the type of $\alpha\psi P$. It is shown that various physical quantities about the IPN can be well explained as topological phenomena.

Appendices
Transformation Matrices

In the several subsections hereafter, including this one, the survey of the preceding topological theories[7~12] will be described as concisely as possible. The interaction among strands plays an important role in the topological theories.[7~12] A word strand means a polymer chain which joins two neighboring junction points. A word junction point means the jointing part of strands in the networks. All of the polymers representing elasticity are regarded as composed of the network which consists of a great number of junction points and strands. In the case of general lattice models, a fundamental unit, which describes the physical properties of the

whole network system, is called a cell. The another important conception of the topological theory is called the GLC(Gauss Linking Coefficient). Let's define $T_{\alpha\beta}$ to be the GLC between loops α and β, and define θ_{ab} to be the GLC between strands a and b as follows:

$$T_{\alpha\beta}=\frac{1}{4\pi}\oint\oint\frac{\{\dot{\rho}_\alpha\times\dot{\rho}_\beta\}\{\rho_\alpha-\rho_\beta\}}{|\rho_\alpha-\rho_\beta|^3}dS_\alpha dS_\beta \tag{A1}$$

$$\theta_{ab}=\int_{r_a}^{r_a'}\int_{r_b}^{r_b'}\frac{\{\dot{\rho}_a\times\dot{\rho}_b\}\{\rho_a-\rho_b\}}{|\rho_a-\rho_b|^3}dS_a dS_b \tag{A2}$$

where ρ_k is a position vector determined by parameter S_k which takes the variation field within the length area of the given segment at any moment. The subscript k is α or β for loops and a or b for strands, and the quantity $\dot{\rho}_k$ is defined as $d\rho_k/dS_k$. Let T_o and θ be the sets of loop and strand GLC's, respectively. Let T_1 be a subset which meets the condition that all elements of T_o should be represented as linear combinations of elements of T_1. Now the transformation matrices between the sets of loop and strand GLC's are given by

$$\begin{aligned}T_o&=\theta C\\ T_1&=T_oB\\ T_1&=\theta\Gamma\\ \Gamma&=CB\end{aligned} \tag{A3}$$

where T_o, T_1, and θ are n_o, n_1, and n_2 dimensional row vectors, respectively, and Γ is $n_2\times n_1$ dimensional matrix. n_o is the number of GLC's of T_o, n_1 is that of GLC's of T_1, and n_2 is that of GLC's of θ.

In the topological theories, the total free energy of the network F may be separated into four terms as follows:

$$F=F_{o,ph}+F_{o,top}+F_1+F_2 \tag{A4}$$

where $F_{o,ph}$ is a term coming from the entropic force acting between the ends of the strands, and $F_{o,top}$ is one coming from the topological interaction among the strands when all the junction points deform affinely. F_1 is a correction term due to nonaffine displacement of the junction points, and F_2 is one due to the fluctuation of θ. The transition matrices of Eq. (A3) contribute only to F_2.

A generalized inverse[15] of any matrix A is defined by

$$A^+\equiv(A'A)^{-1}A' \tag{A5}$$

where A', of course, is a transpose of A, and $(A'A)^{-1}$ is an inverse matrix of $A'A$. The projection matrices of Γ and C are given by, respectively,

$$\begin{aligned}\Gamma^\#&=\Gamma(\Gamma'\Gamma)^+\Gamma'\\ C^\#&=C(C'C)^+C'\end{aligned} \tag{A6}$$

According to proofs[15] of matrix relationships,

$$\begin{aligned}\Gamma^\#&=C^\#\\ Tr\,\Gamma^\#&=Tr\,C^\#=n_1\end{aligned} \tag{A7}$$

where n_1 is the number of the elements of T_1. Alternatively speaking, n_1 is the number of effective loop pairs. $\Gamma^\#$ should be found according to the given model of the network as shown later more clearly.

Distribution Function

Usually, the free energy of networks can be calculated from the distribution functions of junction points and strands. The conditional distribution function $\psi(\tau/r)$ is defined as

$$\psi(\tau/r)=\int_{\tau-1/2}^{\tau+1/2}\int\delta(t-\theta\Gamma)\prod_p[(1-G_p/H_p)\delta(\theta_p)+(G_p/H_p)2\pi H_p)^{-1/2}\cdot\exp(-\theta_p^2/2H_p)]d\theta dt \tag{A8}$$

where δ is a delta function, τ is any element of T_1, r_o is the set of position vectors of junction points in the reference state, and r is the set of those in any state. G_p and H_p are given by, respectively

$$\begin{aligned}G_p(r)&=\nu'^2\gamma g_p(r)\\ H_p(r)&=\nu'^2\gamma h_p(r)\end{aligned} \tag{A9}$$

where γ is a characteristic parameter for the given model, and ν′ is the number of submolecules included in a strand. In Eq. (A9), ρ represents the bond pair of the strands a and b, and r is represented by

$$r=\{r_a,\ r_a',\ r_b,\ r_b'\} \tag{A10}$$

where r_a and r_b' are the position vectors of end points of the strand a, and r_b and r_b' are those of the strand b. Let the letter μ denote the bond pair of the submolecules a_i and b_j, and the letter μ′ that of the submolecules a_i' and b_j'.

When the vector r is fixed, let $P_{ph}(O_\mu|r)$ be the distribution function of single contact obtained when the bond pair μ is formed, and $P_{ph}(O_\mu,\ \mu'|r)$ that of double contact obtained when the bond pairs μ and μ′ are formed between two strands in a phantom network. Then the $g_p(r)$ and $h_p(r)$ in Eq. (A9) are given by

$$\begin{aligned}g_p(r)&=\nu'^{-2}\sum_{\mu=1}^{\nu'^2}P_{ph}(O_\mu|r)\\ h_p(r)&=\nu'^{-2}[g_p(r)]^{-1}\sum_{\mu=1}^{\nu'^2}\sum_{\mu'=1}^{\nu'^2}P_{ph}(O_{\mu,\mu'}|r)\end{aligned} \tag{A11}$$

where $g_p(r)$ is the value of the mean single contact probability and $h_p(r)$ that of the mean double contact one between submolecules in two strands.

Free Energy of the Network

The derivatives of the total free energy of the network F with respect to the macroscopic strain λ can be given as follows:

$$\frac{\partial F}{\partial\lambda}=\frac{\partial F_{o,ph}}{\partial\lambda}+\frac{\partial F_{o,top}}{\partial\lambda}+\frac{\partial F_1}{\partial\lambda}+\frac{\partial F_2}{\partial\lambda} \tag{A12}$$

$$\frac{\partial F_{o,ph}}{\partial\lambda}=3\sum_s\frac{1}{l_s^2}(\dot{r}_s''-\dot{r}_s') \tag{A13}$$

$$\frac{\partial F_{o,top}}{\partial\lambda}=-kT\sum_p\left[\left(\frac{\dot{g}_p^\circ}{g_p^\circ}-\frac{\dot{h}_p^\circ}{h_p^\circ}\right)\left\{\frac{g_p^\circ}{h_p^\circ}-\frac{g_p^\circ(g_p^\circ-h_k^\circ)}{h_p^\circ(g_p^\circ-h_p^\circ)}\right\}+\frac{\dot{h}_p^\circ}{2h_p^\circ}\left(\frac{g_p^\circ}{h_p^\circ}-\frac{g_p^\circ}{g_p^\circ}\right)\right] \tag{A14}$$

$$\frac{\partial F_1}{\partial\lambda}=-\frac{kT}{2}Tr\,(\langle W^*\rangle(\langle W^*\rangle)^+-2\langle\dot{V}^*V^*\rangle(\langle W^*\rangle)^+ +\langle V^*V^*\rangle(\langle W^*\rangle)^+\langle\dot{W}^*\rangle(\langle W^*\rangle)^+) \tag{A15}$$

$$\frac{\partial F_2}{\partial \lambda} = -\frac{kT}{2}\left(\sum_p (\bar{\Gamma}_{pp}{}^*)^2 \frac{h_p^*}{h_p^*}\left(\frac{g_p^\circ}{h_p^\circ} - \frac{g_p^\circ}{h_p^*}\right) + \sum_p \sum_{p'} (\bar{\Gamma}_{pp'}{}^*)^2 \frac{g_p^\circ h_{p'}^*}{(h_p^*)^3} \frac{g_{p'}^\circ h_{p'}^*}{h^\circ{}_{p'}}\right) \quad \text{(A16)}$$

The letter s of Eq. (A13) represents any strand in the network, and l_s^2 is the mean squared end-to-end distance of the strand s in the phantom network. The position vectors of end points in the strand s are expressed as r_s' and r_s. The symbol dot $(\cdot)$ denotes the first derivatives of given functions in regard to λ, such as

$$r_s'' = \frac{\partial r_s''}{\partial \lambda}, \quad r_s^* = \frac{\partial r_s^*}{\partial \lambda}, \quad \dot{g}_p^* = \frac{\partial g_p^*}{\partial \lambda}, \quad \cdots \quad \text{(A17)}$$

where the superscript $\circ$ attached on the g_p and h_p represents that they are the values at $r=r^\circ$ and the superscript $*$ attached on the g_p, h_p, V, W, and etc. denotes that they are the ones at $r=r^*$, r^* being the set of position vectors of junction points deformed affinelikely under the macroscopic strain λ.

Now consider a new function U defined as

$$U = -\ln\phi(\theta, r)|_{\theta=\theta_0} \quad \text{(A18)}$$

where $\phi(\theta, r)$ is the distribution function expressed as

$$V_i^* = \frac{\partial}{\partial r_i} U|_{r=r^*} \quad \text{(A19)}$$

$$W_{ij}^* = \frac{\partial}{\partial r_i}\frac{\partial}{\partial r_j} U|_{r=r^*} \quad \text{(A20)}$$

where V^* is an M_o dimensional super vector whose ith element is V_i^* and W^* is an $M_o \times M_o$ super matrix whose i, j element is W_{ij}^*.

Since the more detailed contents of Eqs. (A12) to (A16) are given by the previous references,[11~12] the detailed description of the above equations is omitted here.

Acknowledgment. The Present Studies were Supported (in part) by the Basic Science Research Institute Program, Ministry of Education, 1994, Project No. BSRI-94-3414.

References

1. Flory, P. J.; Rehner, J. Jr. *J. Chem. Phys.* **1943**, *11*, 521.
2. Edwards, S. F.; Freed, K. F. *J. Phys. C.* **1970**, *3*, 760.
3. Graessley, W. W. *Macromolecules* **1975**, *8*, 865.
4. Ronca, G.; Allegera, G. *J. Chem. Phys* **1975**, *8*, 865.
5. Flory, P. J. *Proc. R. Soc. London Ser. A* **1976**, *351*, 351.
6. Ziabicki, A.; Walasek, *macromolecules* **1978**, *11*, 471.
7. (a) Langley, N. R. *Macromolecules* **1968**, *1*, 348. (b) Langley, N. R.; Polmansteer, K. E. *J. Poly. Sci.* **1974**, *12*, 1023.
8. Deam, R. T.; Edwards, S. F. *Philos, Trans. R. Soc. London Ser. A* **1976**, *280*, 317.
9. Graessley, W. W.; Pearson, D. S. *J. Chem. Phys.* **1977**, *66*, 3363.
10. Iwata, K.; Kurata, M. *J. Chem. Phys.* **1969**, *50*, 4008.
11. Iwata, K. *J. Chem. Phys.* **1980**, *73*, 562; **1981**, *74*, 2039; **1983**, *78*, 2778; **1985**, *83*, 1969.
12. Iwata, K. *J. Chem. Phys.* **1982**, *76*; 6363; **1982**, *ibid* 6375.
13. Son, J. M.; Pak, H. *Bull. Korean Chem. Soc.* **1989**, Vol 10, No. 1, 84.
14. Tsenoglou, C. *J. Polym. Sci.* **1988**, *26*, 2329.
15. Strang, G. *Linear Algebra and its Application*; Academic Press: New York, 1976.
16. Wu, S. *J. Polym. Sci. Polym. Phys. Ed.* **1987**, *25*, 557.
17. Flory, P. J. *Principles of Polymer Chemistry* **1953**, 463, Cornel University, New York.
18. Mancke, R. G.; Dickie, R. A.; Ferry, J. D. *J. Polym. Sci. A-2*, **1968**, *6*, 1783.
19. Sperling, L. H. *Interpenetrating Polymer Networks and Related Materials*, 52, Plenum Press: New York, 1981.
20. Prest, W. M.; Porter, R. S. *J. Polym. Sci., Part A-2* **1972**, *10*, 1639.
21. Wisniewsky, C.; Martin, G.; Monge, P. *Eur. Polym. J.* **1984**, 20, 691.
22. Wu, S. *Polymer* **1987**, *28*, 1144.
23. Wu, S. *Polym. Phys. Ed.* **1987**, *25*, 2511.